O.V. Filonenko, A.G. Grebenyuk, M.I. Terebinska, V.V. Lobanov

QUANTUM CHEMICAL SIMULATION OF ACID-BASE PROPERTIES OF THE SURFACE OF SnO₂ NANOPARTICLES

Chuiko Institute of Surface Chemistry of National Academy of Sciences of Ukraine
17 General Naumov Str., Kyiv, 03164, Ukraine, E-mail: filonenko_ov@ukr.net

Molecular models for tin dioxide nanoparticles containing 1-7 metal atoms and coordinated or constitutive water have been constructed. Dependent on the composition of the models, the coordination number of the tin atom varied from 4 to 6, and that of oxygen was 2 or 3. The considered models contained both terminal (Sn–OH) and bridging (Sn–OH–Sn) hydroxyl groups, and also bridging (Sn–O–Sn) groups. Their equilibrium spatial and electronic structures were calculated using the second-order Møller-Plesset perturbation theory method with the SBKJC valence-only basis set. To assess the gas-phase acidity of the dioxide surface, the deprotonation energy of the studied models was determined. The adsorption energy of water molecules and hydroxide ions on aprotic (incompletely coordinated) tin atoms, which act as Lewis acid centers, was calculated. In order to estimate the pK_a value of the surface of tin dioxide, the Gibbs free energy was calculated for the process of formation of ion pairs due to the proton transfer from hydroxyl groups to adsorbed water molecules. Based on the analysis of the energy effects of the coordination of water molecules and of hydroxide ion, the removal of a proton and its transfer on the hydrated surface of tin dioxide, quantitative estimates have been made of the acid-base characteristics of the active sites of the SnO₂ surface. The dependence of the acidity of hydroxyl groups and coordinated water molecules on the coordination number of the oxygen atom and the neighboring tin atom, as well as on the dimensions of the cluster model, was revealed. It is shown that the acidity of protonic and aprotic sites naturally decreases with an increase in the coordination number of the tin atom. The method of calculating the value of pK_a used in the work for the smallest model of the SnO₂·2H₂O composition allows one to reproduce the experimental data for stannic acids.

Keywords: SnO₂ nanoparticles, Møller-Plesset second order perturbation theory, cluster model, acid-base properties, gas phase acidity, proton transfer

INTRODUCTION

The wide scope of the use of materials based on SnO₂ is due to the combination of a number of unique optical and electrophysical properties. Such materials are non-toxic and economically available. Thus, SnO₂ is used as an anode material in lithium-ion batteries [1, 2], a catalyst for the oxidation of organic compounds [3–5], transparent electrodes of solar batteries, LEDs, and various electronic and optical coatings [6–9]. Today, tin dioxide as a three-dimensional (3D) material is quite well studied. However, various nanostructured types of SnO₂ show better properties compared to bulk ones both for gas analysis and for a wide range of other applications. Therefore, nanoscale materials based on SnO₂ in the form of nanoparticles, nanospheres, nanotubes, nanowires, and nanoribbons are attracting increased interest [10].

Various fields of applications of tin dioxide have led to interest in the construction and systematic analysis of the properties of models for crystals and nanoparticles of this substance to find the structure-property relationship, in particular with the involvement of quantum chemistry methods [11]. In the literature, there are known periodic, i.e., superimposed periodic conditions [12–16] and cluster [17–21] approaches to reproducing the structure and properties of SnO₂. The latter are more convenient for reproducing the properties of tin dioxide nanoparticles, since they have no long-range order. Cluster models are based on the capability to model a nanoparticle or its surface with a small number of atoms. The use of cluster models allows one the use of modern computer programs designed to calculate the properties of molecules, but they require careful selection of the molecular cluster itself.

For the development of highly efficient catalysts and gas sensors, the results of research into the properties of the surface of nanoparticles of tin dioxide and the nature of its active sites are particularly important, because their nature and concentration determine the nature of the

interaction of these nanoparticles with molecules of the gas of the sensing medium.

The active site is a local area on the surface characterized by specific chemical properties. These sites play a key role in the adsorption and reactivity of both solids and nanoparticles due to the presence of dangling bonds and incompletely coordinated surface atoms.

The surface of SnO_2 contains adsorbed water molecules, which, upon dissociation, are capable of forming OH groups of an acidic or basic nature (depending on their coordination environment), incompletely coordinated tin and oxygen atoms, and defective (for metal and oxygen) sites, which can be either protonated or aprotic acid or basic sites [22, 23].

Modern approaches to the theoretical analysis of acid-base characteristics and the corresponding values of pK_a of hydroxyl groups of organic and inorganic substances involve the construction of quantitative "structure-property" relationships with the involvement of the results of experimental and theoretical studies [24]. The aim of the work is to determine the correspondence between the spatial structure and acid-base properties of atomic groups of different nature on the surface of tin dioxide nanoparticles based on the results of systematic quantum chemical calculations of cluster models for probable active sites.

RESEARCH OBJECTS AND METHODS

Calculations were carried out by the Hartree–Fock method with the SBKJC valence-only basis set and respective effective core potential within the PC GAMESS software package (FireFly 8.2.0). Electronic correlation was taken into account using second-order Møller-Plesset perturbation theory. It was shown in [25] that the use of this method gives results that are in good agreement with the experimental ones when calculating the atomic and electronic structure of a number of crystalline oxides, in particular tin dioxide. The equilibrium spatial structures of all clusters considered in the work were found by minimizing the norm of the total energy gradient. The stationarity of the points corresponding to the energy minima of the optimized structures is proved by the absence of negative eigenvalues of the Hessian matrices.

The equilibrium constants of proton transfer reactions of hydroxyl groups of tin dioxide clusters were determined by the formula:

$$\lg K_{react} = -\frac{\Delta G_{react}}{2.303 RT} \quad (pK = \frac{\Delta G_{react}}{2.303 RT}), \qquad (1)$$

where R is the universal gas constant, T is the temperature, and ΔG is the Gibbs free energy of the reaction.

$$\Delta G_{react} = G^0_{298}\ (molecular\ associate) - G^0_{298}\ (ion\ pair), \qquad (2)$$

where $G^0_{298} = E_{tot} + ZPE + G_{0 \to 298\,K}$, E_{tot} is the total energy of optimized structures at 0 K; ZPE is the energy of zero oscillations, which, like the thermodynamic correction $G_{0 \to 298\,K}$, was calculated from the frequencies of normal vibrations obtained by diagonalization of the Hessian matrix of the corresponding optimized structures. When studying proton transfer reactions of hydroxyl groups of tin dioxide clusters, the influence of the aqueous medium was taken into account in the approximation of the continuum solvent model (PCM) within the framework of the US GAMESS program package [26].

In this work, the cluster approximation is used. The calculation of the acidity of the active sites of hydrated tin dioxide nanoparticles was carried out using models for clusters containing from 1 to 7 tin atoms. The equilibrium structures of the considered cluster models of SnO_2 nanoparticles are shown in Fig. 1. The molecule of tin(IV) hydroxide – $Sn(OH)_4 \equiv SnO_2 \cdot 2H_2O$ (Fig. 1 *a*) was chosen as the simplest model. In it, the Sn atom is four-coordinated, and the four oxygen atoms bound to it are two-coordinated. The length of the Sn(IV)–O(II) bonds is 0.194 nm. Since it was necessary to investigate the influence of the coordination number on the properties of the active centers of SnO_2 nanoparticles, the $SnO_5H_6 \equiv SnO_2 \cdot 3H_2O$ (Fig. 1 *b*) and $SnO_6H_8 \equiv SnO_2 \cdot 4H_2O$ (Fig. 1 *c*) clusters were also considered, in which, due to the coordination of the water molecule to the tin atom, the coordination number of the latter increases to 5 and 6, respectively.

As can be seen from the Table 1, the length of the Sn(V)–O(II) and Sn(VI)–O(II) bonds increases with an increase in the coordination number of the tin atom and is 0.198 and 0.199 nm.

Fig. 1 shows the optimized structures of dimers $(SnO_2)_2 \cdot 2H_2O$ (*d*), $(SnO_2)_2 \cdot 4H_2O$ (*e*) and $(SnO_2)_2 \cdot 6H_2O$ (*f*) with coordination numbers of

tin atoms 4, 5 and 6, respectively. In the $(SnO_2)_2 \cdot 4H_2O$ (Fig. 1 *e*) and $(SnO_2)_2 \cdot 6H_2O$ (Fig. 1 *f*) clusters, the bridging oxygen atoms are three-coordinated. In all three cases, a four-membered cycle –Sn–O–Sn–O– is formed in the

dimers, which can be considered as a manifestation of the sign of crystallinity, since such motifs are inherent in the structure of tin dioxide. This leads to lengthening of the Sn–O bonds (see Table 1).
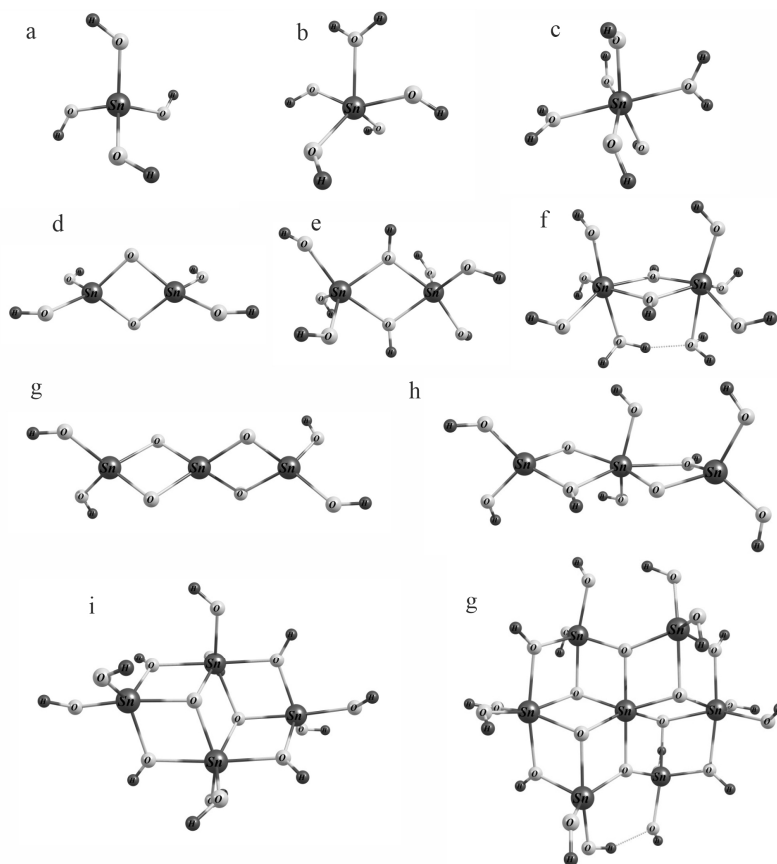

Fig. 1. Optimized structures of hydrated tin dioxide clusters $(SnO_2)_x \cdot yH_2O$ containing from 1 to 7 tin atoms

The presence of two types of bonds with different length values in the formed cycles –Sn–O–Sn–O– indicates the molecular properties of the models. Molecular models are structures in a cluster of which individual molecules can be distinguished based on the difference between intramolecular and intermolecular bonds, which are usually longer. Unlike molecular models, in polyhedral models individual molecules cannot be distinguished because the bond lengths between the same types of atoms are identical.

The length of the coordination bond between the tin and oxygen atoms of the coordinated water molecule in the structures shown in Fig. 1 *b*, *c*, *f* (over 0.22 nm) significantly exceeds the corresponding value for covalent Sn–O bonds (0.194 nm) and coordination bonds

between tin and oxygen atoms, if the latter are characterized by a hypervalent environment (0.198 nm).

For trimers, the stable structures $(SnO_2)_3 \cdot 2H_2O$ (Fig. 1 *g*) and $(SnO_2)_3 \cdot 4H_2O$ (Fig. 1 *h*) were considered. In the first of them (Fig. 1 *g*), all three Sn atoms are four-coordinated, and the oxygen atoms bound to them are two-coordinated. For the cluster (Fig. 1 *h*), the middle tin atom is six-coordinated, and two of the six oxygen atoms around it are three-coordinated.

In clusters $(SnO_2)_4 \cdot 6H_2O$ (Fig. 1 *i*) and $(SnO_2)_7 \cdot 8H_2O$ (Fig. 1 *g*) there are six-coordinated and five-coordinated Sn atoms, two- and three-coordinated O atoms.

From the analysis of the obtained structural parameters of the clusters, it follows that the

length of the Sn–O bond practically does not depend on the size of the cluster and the coordination number of the Sn atoms, but depends on what type of oxygen atoms (two- or three-coordinated) the tin atom is connected to. Namely: Sn–O(III) bond length (($\cong 0.210$ nm) > Sn–O(II) bond length ($\cong 0.198$ nm). The obtained Sn–O(III) bond lengths are in good agreement with the experimental values for SnO₂ crystalline samples (0.205 nm) [10]. For nanoparticles, experimentally measured bond lengths range from 0.191 to 0.216 nm [27]. Based on the calculations, it can be assumed that larger length values correspond to Sn–O bonds located in the bulk (Sn–O–Sn fragment), and smaller values to edge Sn–O bonds (Sn–O–H fragment).

Table 1. Sn–O bond lengths (nm) of equilibrium configurations of stannous dioxide nanoclusters $(SnO_2)_x \cdot yH_2O$

	$d\,(Sn^{IV} - O^{II})$	$d\,(Sn^V - O^{II})$	$d\,(Sn^V - O^{III})$	$d\,(Sn^{VI} - O^{II})$	$d\,(Sn^{VI} - O^{III})$
$SnO_2 \cdot 2H_2O$	0.194				
$SnO_2 \cdot 3H_2O$		0.198	0.220(-Sn-OH₂)		
$SnO_2 \cdot 4H_2O$				0.199	0.224 (–Sn–OH₂)
$(SnO_2)_2 \cdot 2H_2O$	0.194; 0.203(in a cycle –Sn–O–Sn–O–)				
$(SnO_2)_2 \cdot 4H_2O$		0.196	0.206 0.216		
$(SnO_2)_2 \cdot 6H_2O$				0.199	0.208 0.212 0.226 (–Sn–OH₂)
$(SnO_2)_3 \cdot 2H_2O$	0.194; 0.203(in a cycle –Sn–O–Sn–O–)				
$(SnO_2)_3 \cdot 4H_2O$	0.194			0.198	0.203 0.224
$(SnO_2)_4 \cdot 6H_2O$		0.196	0.204 0.208	0.197	0.212 0.222
$(SnO_2)_7 \cdot 8H_2O$		0.196	0.202 0.214	0.197	0.210 0.219
Exp.					0.205 (cryst.) [10] 0.196 – 0.216 (nanopart.)[27]

As is known [23], there are two types of acid sites on the surface of SnO₂: Lewis (strong) and Brønsted (weak). The so-called Lewis acids (acid centers of the aprotic type) are coordinatively unsaturated (four- and five-coordinated) tin atoms that can exist on its surface (Fig. 2 *a*).

Brønsted centers are acid centers of the proton type, namely, neutral hydroxyl groups on the surface of tin hydroxide, protonated hydroxyl groups and protonated bridging oxygen atoms formed on the surface due to the addition or dissociation of water molecules (Fig. 2 *b*).

Different models for possible acid sites of aprotic and protonic type are considered. Their acidity was evaluated in three ways:

1) to estimate the gas-phase acidity, the deprotonation energy of the studied models was calculated (Table 2);

2) calculated the adsorption energy of water molecules and hydroxide ions on aprotic (incompletely coordinated) tin atoms (Tables 3, 4);

3) calculated the change in the Gibbs free energy of the formation of ion pairs on the surface of hydrated SnO₂ nanoparticles due to proton transfer from surface hydroxyl groups to adsorbed water molecules.

From the analysis of the obtained energies of gas-phase deprotonation of the above models of hydrated tin dioxide $(SnO_2)_x \cdot yH_2O$ (Table 2), it follows that:

1) the acidity of hydroxyl groups gradually increases with increasing cluster size and depends on the coordination number of tin atoms;

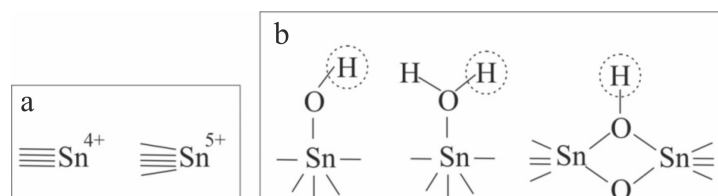2) when the Sn–OH group is coordinated to the neighboring tin atom, its acidity increases.

Fig. 2. Considered models of aprotic (*a*) and protonic (*b*) acid sites that can exist on the surface of tin dioxide nanoparticles

Table 2. Energy of gas-phase deprotonation (kJ/mol) of terminal and bridging hydroxyl groups of hydrated tin dioxide clusters $(SnO_2)_x \cdot yH_2O$

Coordination number of an atom Sn		x=1	x=2	x=3	x=4	x=7
4	-OH	1443.6 (Fig. 1 *a*)	1379.9 (Fig. 1 *d*)	1360.6 (Fig. 1 *g*)		
5	-OH	eliminate H₂O (Fig. 1 *b*)	1420.2 (Fig. 1 *e*)		1407.9 (Fig. 1 *g*)	1360.9 (Fig. 1 *k*)
6	-OH	eliminate H₂O (Fig. 1 *c*)	eliminate H₂O (Fig. 1 *f*)	1415.0 (Fig. 1 *h*)	1450.4 (Fig. 1 *g*)	-
	-SnOHSn		1332.1 (Fig. 1 *e*)	1295.1 (Fig. 1 *h*)	1322.6 (Fig. 1 *g*)	1282.0 (Fig. 1 *k*)

The deprotonation energy of water molecules coordinated to the tin atom in the cases of Figures 1 *b* and 1 *f* is 1356.2 and 1358.0 kJ/mol, respectively. As we can see, the acidity of OH₂ groups is higher than that of Sn–OH groups.

Therefore, for the considered structures, the acidity increases in the order Sn–OH < Sn–OH–Sn < Sn–OH₂. This is in good agreement with the experimental results obtained in [28]. Therein, using the method of infrared spectroscopy combined with the diffuse reflectance technique (DRIFT), it is shown that on the surface of SnO₂ nanocrystalline samples, bridged hydroxyl groups Sn–OH–Sn are more acidic than terminal Sn–OH groups.

The energy of coordination of water molecules and hydroxide anion increases with the increase in the size of the cluster. An increase in the coordination number of the tin atom reduces its capability to bind water molecules and hydroxide anion (see Tables 3, 4).

Table 3. Energy of gas-phase hydration (kJ/mol) of hydrated tin dioxide clusters $(SnO_2)_x \cdot yH_2O$

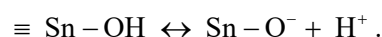| Coordination number of Sn atom	x = 1	x = 2	x = 3	x = 4	x = 7
4	-88.16	-99.96	-98.65		
5	-33.58	-49.85	-64.81	-67.43	-97.34

Table 4. Energy of gas-phase adsorption (kJ/mol) of OH⁻ anion on hydrated tin dioxide clusters $(SnO_2)_x \cdot yH_2O$

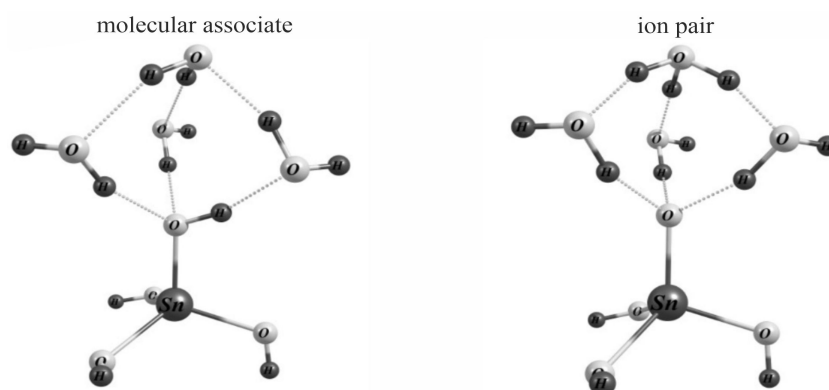| Coordination number of an atom Sn	x = 1	x = 2	x = 3	x = 4	x = 7
4	-418.75	-483.29	-523.17	-	-
5	-	-452.60	-	-520.03	-533.93

The results obtained in the work regarding the adsorption energies of water molecules and hydroxide ions on incompletely coordinated tin atoms are in good agreement with the experimental ones. For example, in work [29], investigating the chemisorption of NH₃ on the SnO₂ (110) face using the methods of thermal desorption and UV photoelectron spectroscopy, it was shown that four-coordinated tin atoms are stronger acid sites compared to five-coordinated ones.

In the paper, the thermodynamic characteristics of the proton transfer reaction from the Sn(OH)₄ molecule to the water molecules of the hydrate shell and the equilibrium constant pK_a of this process are calculated. The deprotonation reaction of Sn–OH groups is considered, as an example, for the simplest model (Sn(OH)₄) of hydrated SnO₂ nanoparticles. It can be represented by the following scheme:

$$\equiv Sn-OH \leftrightarrow Sn-O^- + H^+ .$$

The molecule $Sn(OH)_4 \equiv H_4SnO_4 \equiv SnO_2 \cdot 2H_2O$ is orthostannic acid; it can be considered as a precursor in the synthesis of hydrated tin dioxide nanoparticles. In [30], experimental values of the acid dissociation constant of surface hydroxyl groups of samples of hydrated tin dioxide obtained during acid or alkaline hydrolysis of tin(IV) salts are given, which is equal to 7.6 (regardless of the method of synthesis).

Fig. 3. Spatial structure of cluster models of adsorption complexes of water with the Sn(OH)₄ cluster

Table 5. Values of change in total energy (ΔE_{react}), Gibbs free energy (ΔG_{react}) of deprotonation of Sn(OH)₄ hydroxyl group and theoretical and experimental dissociation constants pK_a Sn–OH for stannic acid groups

Method of calculation	ΔE_{react}	ΔG_{react}	pK_a
MP2/RHF/SBKJC	9.4	18.9	3.3
MP2/RHF/SBKJC/PCM	24.9	27.4	4.8
MP2/RHF/SBKJC(d,p)	32.3	39.6	6.9
MP2/RHF/SBKJC++(d,p)	38.0	39.2	6.9
MP2/RHF/SBKJC(d,p)/PCM	37.5	42.7	7.5
Exp [29]			7.6

Modeling of the protolytic equilibrium of the Sn–OH group of the Sn(OH)$_4$ cluster was carried out by calculating the change in the value of the Gibbs free energy, an inherent charge separation reaction in a complex with four water molecules (Fig. 3). As shown in works [31–33], this approach gives results that are consistent with the experiment for clusters of silicon dioxide and orthosilicate acid. Fig. 3 shows two states: molecular (*a*) and with separated charges (*b*). When the latter is formed, a proton is transferred from the Sn–OH group to water molecules with the formation of a hydroxonium ion, which, together with the oxygen atom of the deprotonated stanol group, is located at the opposite vertices of the trigonal bipyramid and is separated by three water molecules.

The value of pK_a within the framework of the used model was calculated using various basis sets and methods, in particular, within the PCM model for the solvent (Table 5). It follows from the obtained data that the calculations using the MP2/RHF/SBKJC(d,p)/PCM method give the closest to the experimental value of pK_a (SnO$_2$·2H$_2$O).

CONCLUSIONS

Cluster models of proton-donating and aprotic acid sites on the surface of tin dioxide have been constructed. It is shown that the general regularities of changes in the acid-base characteristics of the surface of the state dioxide dependent on the coordination environment of the active sites can be correctly reproduced with the help of relatively small molecular models.

The acidity of protonic and aprotic centers naturally decreases with an increase in the coordination number of the tin atom. The calculated deprotonation energy values are correlated with experimental data on the acidity of different types of hydroxyl groups on the surface.

The method of calculating the value of pK_a for the smallest model used in the work allows one to reproduce the experimental data for stannic acids.

Квантовохімічне моделювання кислотно-основних властивостей поверхні наночастинок SnO$_2$

О.В. Філоненко, А.Г. Гребенюк, М.І. Теребінська, В.В. Лобанов

Інститут хімії поверхні ім. О.О. Чуйка Національної академії наук України
вул. Генерала Наумова, 17, Київ, 03164, Україна, filonenko_ov@ukr.net

Побудовано молекулярні моделі наночастинок діоксиду станума, які містять 1-7 атомів металу і можуть включати координовану або конституційну воду. В залежності від складу моделей, координаційне число атома Станума змінювалось від 4 до 6, а Оксигену – становило 2 або 3. Розглянуті моделі містили як термінальні (Sn–OH), так і місткові (Sn–OH–Sn) гідроксильні групи, а також місткові (Sn–O–Sn) групи. Методом теорії збурень Меллера-Плессета другого порядку з валентним базисним набором SBKJC та відповідним ефективним остовним потенціалом розраховано їхню рівноважну просторову та електронну будову. Для оцінки газофазної кислотності поверхні діоксиду станума визначено енергію депротонування досліджуваних моделей. Розраховано енергію адсорбції молекул води та гідроксид-іонів на апротонних (неповнокоординованих) атомах Станума, які виступають в ролі кислотних центрів Льюїса. З метою оцінки величини pK$_a$ поверхні діоксиду станума розраховано вільну енергію Гіббса для процесу утворення іонних пар завдяки перенесенню протона від гідроксильних груп до адсорбованих молекул води. На підставі аналізу енергетичних ефектів координації молекул води та гідроксид-іона, видалення протона та його перенесення на гідратованій поверхні діоксиду станума зроблено кількісні оцінки кислотно-основних характеристик активних центрів поверхні SnO$_2$. Виявлено залежність кислотності гідроксильних груп та координованих молекул води від координаційного числа атома Оксигену та сусіднього атома Станума, а також від розмірів кластерної моделі. Показано, що кислотність протонних та апротонних центрів залежить від їхнього оточення та закономірно зменшується при збільшенні координаційного числа атома Станума. Використана в роботі методика розрахунку величини pK$_a$ для найменшої моделі складу SnO$_2$·2H$_2$O дозволяє відтворити експериментальні дані для станатних кислот.

***Ключові слова**: наночастинки SnO$_2$, теорія збурень Меллера-Плессета другого порядку, кластерна модель, кислотно-основні властивості, газофазна кислотність, перенесення протона*

REFERENCES

1. Lee S.-Y., Park K.-Y., Kim W.-S., Yoon S., Hong S.-H., Kang K., Kim M. Unveiling origin of additional capacity of SnO_2 anode in lithium-ion batteries by realistic ex situ TEM analysis. *Nano Energy*. 2016. **19**: 234.
2. Odani A., Nimberger A., Markovsky B., Sominski E., Levi E., Kumar V.G. Development and testing of nanomaterials for rechargeable lithium batteries. *J. Power Sources*. 2003. **119–121**: 517.
3. Xu X., Zhang R., Zeng X., Han X., Li Y., Liu Y., Wang X. Effects of La, Ce, and Y oxides on SnO_2 catalysts for CO and CH_4 oxidation. *Chem. Cat. Chem*. 2013. **5**(7): 2025.
4. Liberkova K., Touroude R. Performance of Pt/SnO_2 catalyst in the gas phase hydrogenation of crotonaldehyde. *J. Mol. Catal. A Chem*. 2002. **180**(1–2): 221.
5. Manjunathan P., Marakatti V.S., Chandra P., Kulal A.B., Umbarkar S.B., Ravishankar R. Mesoporous tin oxide: an efficient catalyst with versatile applications in acid and oxidation catalysis. *Catal. Today*. 2018. **309**: 61.
6. Ray S., Dutta J., Barua A.K. Bilayer SnO_2: In/SnO_2 thin films as transparent electrodes of amorphous silicon solar cells. *Thin Solid Films*. 1991. **199**(2): 201.
7. Tran V.-H., Ambade R.B., Ambade S.B., Lee S.-H., Lee I.-H. Low-temperature solution-processed SnO_2 nanoparticles as a cathode buffer layer for inverted organic solar cells. *ACS Appl. Mater. Interfaces*. 2017. **9**(2): 1645.
8. Valitova I., Natile M.M., Soavi F., Santato C., Cicoira F. Tin dioxide electrolyte-gated transistors working in depletion and enhancement modes. *ACS Appl. Mater. Interfaces*. 2017. **9**(42): 37013.
9. Granqvist C.G. Transparent conductors as solar energy materials: A panoramic review. *Sol. Energy Mater. Sol. Cells*. 2007. **91**(17): 1529.
10. *Tin Oxide Materials. Synthesis, Properties, and Applications*. (Elsevier Inc. 2020).
11. Sauer J. Molecular models in ab initio studies of solids and surfaces: from ionic crystals and semiconductors to catalysts. *Chem. Rev.* 1989. **89**(1): 199.
12. Oviedo J., Gillan M.J. Energetics and structure of stoichiometric SnO_2 surfaces studied by first-principles calculations. *Surf. Sci*. 2000. **463**(2): 93.
13. Hong S.-N., Kye Y.-H., Yu C.-J., Jong U.-G., Ri G.-C., Choe C.-S., Han J.-M. Ab initio thermodynamic study of the SnO_2 (110) surface in an O_2 and NO environment: a fundamental understanding of the gas sensing mechanism for NO and NO_2. *Phys. Chem. Chem. Phys*. 2016. **18**(46): 31566.
14. Agamalyan M.A., Hunanyan A.A., Harutyunyan V.M., Aleksanyan M.S., Sayunts A.G., Zakaryan A.A. Studies of the interaction of H_2O_2 with the SnO_2 (110) surface from first principles. *Izvestia of the National Academy of Sciences of Armenia, Phys*. 2020. **55**(3): 358. [in Russian].
15. Korotcenkov G., Golovanov V., Brinzari V., Cornet A., Morante J., Ivanov M. Distinguishing feature of metal oxide films' structural engineering for gas sensor applications. *J. Phys*. 2005. **15**: 256.
16. Kılıç C., Zunger A. Origins of coexistence of conductivity and transparency in SnO_2. *Phys. Rev. Let*. 2002. **88**(9): 95.
17. Sensato F.R., Filho O.T., Longo E., Sambrano J.R., Andres J. Theoretical analysis of the energy levels indused by oxygen vacancies and the doping process (Co, Cu and Zn) on SnO_2 (110) surface models. *J. Mol. Struct*. 2001. **541**(1–3): 69.
18. Abdulsattar M.A., Abed H.H., Jabbar R.H., Almaroof N.M. Effect of formaldehyde properties on SnO_2 clusters gas sensitivity: A DFT study. *J. Mol. Graph. Model*. 2021. **102**: 107791.
19. Zhao Z., Li Z. First-principle calculations on the structures and electronic properties of the CO-adsorbed $(SnO_2)_2$ clusters. *Struc. Chem*. 2020. **31**(5): 1861.
20. Ducere J.-M., Hemeryck A., Esteve A., Rouhani M.D., Landa G., Menini P., Tropis C., Maisonnat A., Fau P., Chaudret B. A Computational chemist approach to gas sensors: modeling the response of SnO_2 to CO, O_2, and H_2O gases. *J. Comput. Chem*. 2011. **33**(3): 247.
21. Tingting S., Fuchun Z., Weihu Z. Density functional theory study on the electronic structure and optical properties of SnO_2. *Rare Metal Materials and Engineering*. 2015. **44**(10): 2409.
22. Tanabe K. *Solid Acids and Bases: Their Catalytic Properties*. (Tokyo: Kodansha Ltd., 1970.)
23. Marikutsa A.V., Rumyantseva M.N., Konstantinova E.A., Shatalova T.B., Gaskov A.M. Active sites on nanocrystalline tin dioxide surface: effect of palladium and ruthenium oxides clusters. *J. Phys. Chem. C*. 2014. **118**(37): 21541.
24. Baldasare C.A., Seybold H.G. Computational Estimation of the Aqueous Acidities of Alcohols, Hydrates, and Enols. *J. Phys. Chem. A*. 2021. **125**(17): 3600.
25. Tingting S., Fuchun Z., Weihu Z. Density functional theory study on the electronic structure and optical properties of SnO_2. *Rare Metal Materials and Engineering*. 2015. **44**(10): 2409.

26. Schmidt M.W., Baldridge K.K., Boatz J.A., Elbert S.T., Gordon M.S., Jensen J.H., Koseki S., Matsunaga N., Nguen K.A., Su S.J., Windus T.L., Dupuis M., Montgomery J.A. General atomic and molecular electronic structure system. *J. Comput. Chem.* 1993. **14**(11): 1347.

27. Sain S., Kar A., Patra A., Pradhan S.K. Structural interpretation of SnO₂ nanocrystals of different morphologies synthesized by microwave irradiation and hydrothermal methods. *Cryst. Eng. Comm*. 2014. **16**(6): 1079.

28. Pavelko R.G., Daly H., Hardacre C., Vasilieva A.A., Llobeta E. Interaction of water, hydrogen and their mixtures with SnO₂ based materials: the role of surface hydroxyl groups in detection mechanisms. *Phys. Chem. Chem. Phys.* 2010. **12**: 2639.

29. Abee M.W., Cox D.F. NH₃ chemisorption on stoichiometric and oxygen-deficient SnO₂(110) surfaces. *Surf. Sci.* 2002. **520**(1–2): 65.

30. Petro N.S., El-Naggar I.M., Shabana E.-S.I., Misak N.Z. On the behaviour of hydrous tin oxide as an ion exchanger: structural features, porous texture, capacity and apparent pK values. *Colloids Surf.* 1990. **49**: 219.

31. Demianenko E., Ilchenko M., Grebenyuk A., Lobanov V. A theoretical study on orthosilicic acid dissociation in water clusters. *Chem. Phys. Lett.* 2011. **515**(4–6): 274.

32. Kravchenko A.A., Demianenko E.M., Filonenko O.V., Grebenyuk A.G., Lobanov V.V., Terets M.I. A quantum chemical analysis of dependence of the protolytic properties of silica nanoparticles on the composition and spatial structures of their molecules. *Surface.* 2017. **9(24)**: 28.

33. Grebenyuk A.G. Coexistence of ion pairs and molecular associates in the nanoparticles of inorganic compounds. *Surface.* 2019. **11(26)**: 344. [in Ukrainian].